

Analysis of incoherent scatter radar data from non-thermal *F*-region plasma

K. SUVANTO

Blackett Laboratory, Imperial College, London SW7 2BZ, U.K.

M. LOCKWOOD,* K. J. WINNER, A. D. FARMER and B. J. I. BROMAGE

Rutherford Appleton Laboratory, Chilton, Didcot OX11 0QX, U.K.

(Received in final form 22 March 1989)

Abstract—A procedure is presented for fitting incoherent scatter radar data from non-thermal *F*-region ionospheric plasma, using theoretical spectra previously predicted. It is found that values of the shape distortion factor D^* , associated with deviations of the ion velocity distribution from a Maxwellian distribution, and ion temperatures can be deduced (the results being independent of the path of iteration) if the angle between the line-of-sight and the geomagnetic field is larger than about $15\text{--}20^\circ$. The procedure can be used with one or both of two sets of assumptions. These concern the validity of the adopted model for the line-of-sight ion velocity distribution in the one case or for the full three-dimensional ion velocity distribution function in the other. The distribution function employed was developed to describe the line-of-sight velocity distribution for large aspect angles, but both experimental data and Monte Carlo simulations indicate that the form of the field-perpendicular distribution can also describe the distribution at more general aspect angles. The assumption of this form for the line-of-sight velocity distribution at a general aspect angle enables rigorous derivation of values of the one-dimensional, line-of-sight ion temperature. With some additional assumptions (principally that the field-parallel distribution is always Maxwellian and there is a simple relationship between the ion temperature anisotropy and the distortion of the field-perpendicular distribution from a Maxwellian), fits to data for large aspect angles enable determination of line-of-sight temperatures at all aspect angles and hence, of the average ion temperature and the ion temperature anisotropy. For small aspect angles, the analysis is restricted to the determination of the line-of-sight ion temperature because the theoretical spectrum is insensitive to non-thermal effects when the plasma is viewed along directions almost parallel to the magnetic field. This limitation is expected to apply to any realistic model of the ion velocity distribution function and its consequences are discussed. Fit strategies which allow for mixed ion composition are also considered. Examples of fits to data from various EISCAT observing programmes are presented.

1. INTRODUCTION

The ion velocity distribution in the *F*-region ionosphere may deviate from the Maxwellian shape under the joint action of a supersonic ion drift through the neutral gas and ion-neutral collisions (see e.g. ST.-MAURICE and SCHUNK, 1979, and references cited therein). The distorted distribution function gives rise to characteristic spectra of signals received by an incoherent scatter radar, as predicted by RAMAN (1980) and RAMAN *et al.* (1981), for the magnetic field-dominated case where the ion velocity distribution is gyrotropic. LOCKWOOD *et al.* (1987, 1988, 1989a) were able to identify such spectral signatures in data from EISCAT observations by the U.K. Special Programme experiment POLAR. These authors studied various flow burst events in the dayside auroral oval,

which SIBECK *et al.* (1989) have attributed to the effects of solar wind dynamic pressure changes impinging upon the magnetosphere, but which could also be ionospheric signatures of flux transfer events at the magnetopause (TODD *et al.*, 1986). Recently, LOCKWOOD *et al.* (1989b) have provided strong evidence that other flow burst events are the ionospheric effects of flux transfer events, and the non-thermal plasma they produce is studied in Section 3.2. of this paper. Using the sudden nature of the velocity changes during these events, LOCKWOOD *et al.* (1987, 1988, 1989a) showed that the (apparent) rises in ion temperature, deduced by using the standard Maxwellian interpretation, were too high for the plasma to be bi-Maxwellian.

RAMAN (1980) and RAMAN *et al.* (1981) showed that the form of the spectrum scattered from non-thermal plasma depends upon the aspect angle of the observations, ϕ , i.e. the angle between the geo-

* Also Visiting Honorary Lecturer, Blackett Laboratory, Imperial College, London SW7 2BZ, U.K.

magnetic field and the radar line-of-sight. (For monostatic observations the line-of-sight is the beam direction and for multistatic observations it is the bisector of the transmitter and receiver beams.) WINSER *et al.* (1987, 1989) used the EISCAT latitude scanning Common Programme CP-3-E to show that the aspect angle dependence of the spectral shape was similar to the predictions by RAMAN *et al.* (1981). MOORCROFT and SCHLEGEL (1988) attempted to fit spectra from an earlier version of this programme (CP-3-C) with allowance for non-thermal effects, and the fit variances were found to be somewhat smaller than for the Maxwellian analysis. The anti-correlation of the ion and electron temperatures, obtained if the standard analysis (which assumes a Maxwellian ion velocity distribution) is used, has been cited by several authors as evidence for non-thermal plasma (WINSER *et al.*, 1987, 1989; MOORCROFT and SCHLEGEL, 1988; LOCKWOOD *et al.*, 1988, 1989a).

The procedure employed by MOORCROFT and SCHLEGEL (1988) made use of the RAMAN (1980) computational procedure, with modifications to avoid repetition of one of the three cumbersome numerical integrals (D. Moorcroft, private communication). In this paper we employ the procedure of SUVANTO (1988), which not only avoids repeating this numerical integral but also carries out the other two analytically. This makes the procedure considerably faster and also much less likely to fail to converge on a fit. Furthermore, the Suvanto algorithm is readily generalised to allow for a multi-species ion gas, whereas Moorcroft and Schlegel assumed only O^+ ions were present. This is an important consideration because the large drifts which drive the plasma non-thermal also cause major increases in the molecular ion concentrations (e.g. BUCHERT and LA HOZ, 1988).

In this paper, we will concentrate on technical aspects of non-Maxwellian spectral analysis. Section 2 includes a discussion of the spectral synthesis algorithm and the fitting procedure. The finite Debye length effect for Maxwellian plasma, which has been used to test the algorithm, is compared with the corresponding effect in the case of a non-Maxwellian ion velocity distribution. In Section 3 some examples are presented for observations made using the EISCAT POLAR and Common Programme CP-4 experiments for which the aspect angle remained large ($\sim 72^\circ$) and fixed for each range gate. In Section 4, we study the limitations placed on the analysis by a small value of the aspect angle, with examples from observations by the EISCAT Common Programme CP-3-E. Different fit strategies are also discussed. Finally, we summarise our results in Section 5.

2. THEORETICAL SPECTRA AND THE FITTING PROCEDURE

RAMAN (1980) performed a limited parametric study of the shape of the incoherent scatter spectrum for cases of a supersonic ion drift through the neutral gas in the *F*-region (i.e. the drift of the ions relative to the neutral gas exceeds the thermal speed of the neutrals). An ion velocity distribution function based on the work by ST.-MAURICE and SCHUNK (1979) was employed to model the deviation of the ion population from thermal equilibrium. The functional form of the distribution function actually originates from the use of a simple relaxation model for ion-neutral collisions. However, the observations made using the Retarding Potential Analyser (RPA) on the AE-C satellite (ST.-MAURICE *et al.*, 1976) and Monte Carlo simulations (BARAKAT *et al.*, 1983) have shown that this closed-form solution of the kinetic equation can be used to approximate the real distribution function, at least in the field-perpendicular direction, provided the two parameters on which the distribution function depends, D' (the ratio of the ion drift velocity relative to the neutral gas, to the neutral thermal speed) and T_n (the neutral temperature), are replaced by adjustable empirical parameters termed D^* and T^* by RAMAN (1980). It has recently been pointed out (KIKUCHI *et al.*, 1988; LOCKWOOD and WINSER, 1988) that the form of the distribution function could be further generalised, either by allowing for a field-parallel ion temperature independent of the parameters D^* and T^* , or by using the field-perpendicular part of the original distribution in any direction. The reason for the latter approach is that Monte Carlo simulations of the kind made by BARAKAT *et al.* (1983) indicate that the field-parallel velocity distribution may not remain exactly Maxwellian. In this paper, however, we do not attempt to take advantage of these generalisations: the distribution function employed by RAMAN (1980) and RAMAN *et al.* (1981) will be used. It is clear from the Monte Carlo simulations that several of the major features of this distribution function are valid, including the facts that the deformation of the line-of-sight velocity distribution from a Maxwellian is much greater in the field-perpendicular direction than that in the field-parallel direction and that field-perpendicular ion temperature exceeds the field-parallel value. As a result, the conclusions we reach about the limits to the use of the Raman distribution function do underline general principles, which will also apply, to some extent, to other realistic forms for the distribution function.

The theoretical distribution function differs from a Maxwellian in two ways. First, the field-perpendicular

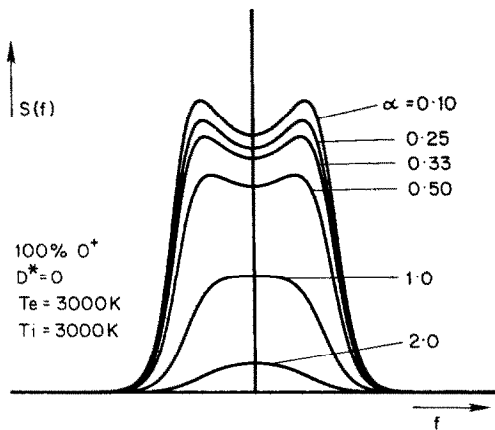


Fig. 1. Finite Debye length effect on the scatter spectrum in the case of a Maxwellian O^+ ion velocity distribution ($D^* = 0$) with $T_e = T_i = 3000$ K. The spectra are shown for various values of $\alpha = 4\pi\lambda_D/\lambda$, where λ_D is the electron Debye length and λ is the radar wavelength, and were evaluated using the SUVANTO (1988) procedure in the thermal limit.

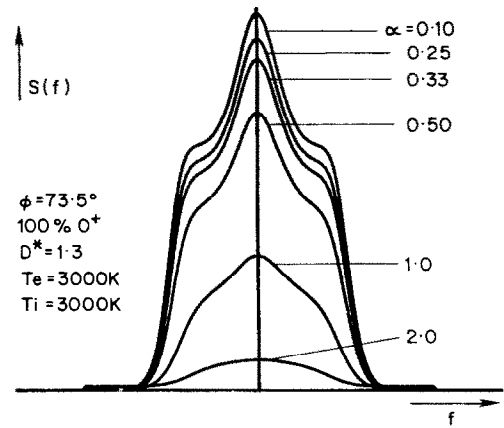


Fig. 2. The same as Fig. 1, but for a highly non-Maxwellian ion velocity distribution ($D^* = 1.3$) viewed at the aspect angle of $\phi = 73.5^\circ$. Note that for $\alpha = 2.0$ the spectra in Figs. 1 and 2 are almost identical but the difference between thermal and non-thermal plasma is clear as soon as collective plasma effects have become important ($\alpha \sim 1$).

distribution is distorted from the Maxwellian shape. Second, temperature in the strict thermodynamic sense does not exist: kinetic temperatures, which may be defined to correspond to random ion motions at different angles with respect to the magnetic field, are not equal. A full discussion of this topic has been given, e.g. by RAMAN (1980) and RAMAN *et al.* (1981) and will not be repeated here. However, it should be noted that as a result of the form of the distribution function which we adopt here (i.e. that given by RAMAN *et al.*, 1981) not only is the field-parallel ion velocity distribution always Maxwellian, but the temperature anisotropy, i.e. the ratio of the field-perpendicular and field-parallel temperatures, is $(1 + D^{*2})$ (see LOCKWOOD and WINNER, 1988).

The synthesised incoherent scatter spectra in this paper are based on the kinetic theory approach by RAMAN (1980). The computational method discussed by SUVANTO (1988), which has been tested in the Maxwellian limit ($D^* = 0$) and also against predictions by RAMAN (1980), is used to produce the theoretical spectra. The SUVANTO (1988) formulation is used, instead of that by RAMAN (1980), because: it is analytic (and does not require a triple numerical integral); it gives an exact, rigorous solution; the variables have been separated to avoid unnecessary repetition of computations. Hence, relatively rapid calculation of each spectrum is achieved. All these factors give considerable advantages when iterating the spectra to fit observations. Figures 1 and 2 show the Debye length (λ_D) effect on the spectrum in the well-known Maxwellian case (the plots of Fig. 1 are identical to

those given by EVANS, 1969) and for a non-Maxwellian ion velocity distribution, respectively, calculated using the Suvanto procedure. Note that for the largest value of α ($= 4\pi\lambda_D/\lambda$ for monostatic radar operation at a wavelength λ), the spectra of Figs. 1 and 2 are very similar, owing to the fact that the scattering is from individual electrons rather than collective density fluctuations of the plasma and, consequently, the form of the ion velocity distribution is not important in this limit. In the transition region corresponding to $\alpha \sim 1$, the features which are characteristic of thermal and non-thermal plasma appear, and spectra associated with non-Maxwellian plasma can be identified by the central peak, as opposed to the double-humped shape, typical of thermal plasma.

The spectral synthesis algorithm of SUVANTO (1988) has been generalised to allow for two ion species. This revised version of the procedure has been tested against previously published spectra for a mixture of thermal O^+ and H^+ or He^+ ions (e.g. MOORCROFT, 1964) and for non-thermal O^+ and NO^+ ions (RAMAN, 1980). We have also carried out tests for a mixture of O^+ and NO^+ ions in the Maxwellian limit, by comparison with results from the spectral synthesis routines in the standard EISCAT programme (LEJEUNE, 1979). In all tests, the routines gave identical spectra, to within computational rounding errors. An example of how the ion composition affects the spectrum is shown in Fig. 3. The O^+ velocity distribution has been chosen to be more distorted from a Maxwellian than the NO^+ distribution as observed by ST.-MAURICE *et al.* (1976) and discussed by ST.-MAURICE

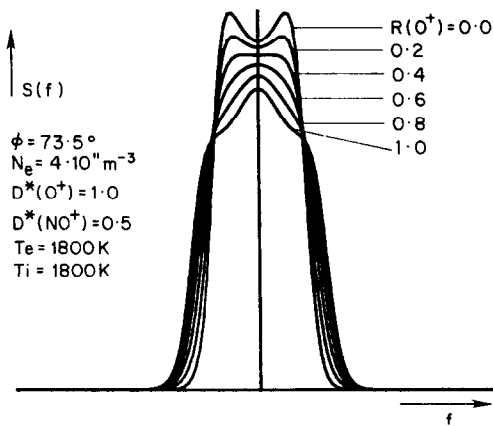


Fig. 3. The effect of ion composition, $R(O^+) = N(O^+)/N_e$, on the scatter spectrum for highly non-Maxwellian O^+ ions and slightly non-Maxwellian NO^+ ions [$D^*(O^+) = 1.3$ and $D^*(NO^+) = 0.50$] with $N_e = 4 \times 10^{11} \text{ m}^{-3}$ and $T_e = T_i = 1800 \text{ K}$.

and SCHUNK (1979). It can be seen that as the ion mass decreases the spectrum width decreases, as in the case of mixed species thermal plasma. However, when the plasma is pure NO^+ [$R(O^+) = 0$] the spectrum appears (at least visually) to be very similar to that for a single species Maxwellian plasma, on account of the low $D^*(NO^+)$ value. When the plasma is pure O^+ [$R(O^+) = 1$], the spectrum is of the single peaked form shown in Fig. 2, because of the higher value for $D^*(O^+)$. At intermediate values of $R(O^+)$, the spectra evolve smoothly between these two limits, with a 'flat-topped' spectrum at $R(O^+) = 0.4$ and a 'bullet' shape (very similar to that for very high temperature Maxwellian ions) for $R(O^+) = 0.6$. The exact nature of this evolution of spectral shape depends on the ratio of electron and ion temperatures and also on the plasma density (via the Debye length effect discussed above).

The non-Maxwellian analysis procedure, illustrated by Fig. 4 for the single species case (the multiple species case is identical in principle), can be divided into two parts. The first part includes the calculation of the coefficients $A_k(p)$ and $dA_k(p)$ needed in the evaluation of the theoretical ion velocity distribution function and its slope. (For definitions of the symbols appearing in Fig. 4 the reader is referred to the paper by SUVANTO, 1988.) These computations are very time-consuming but do not need to be repeated until data for a different aspect angle (ϕ) are selected. The actual iterative fitting procedure then follows. The initial value of D^* , D_0^* , is arbitrarily specified and the initial values of N_e , T_e and T_i are taken from an

approximate 'quick fit' to the data (based on the assumption of a Maxwellian plasma). The model spectrum is computed for various sets of values for the plasma parameters which are iterated until an agreement with the observed spectrum is obtained. Note that fitting is actually carried out in the time domain, i.e. on the Fourier transform of the spectrum, the autocorrelation function. convergence to a fit is attained somewhat less often than for Maxwellian plasma analysis, especially when the signal-to-noise ratio is low. The principal reason for this is that an observed spectrum is ambiguous and can be fitted with two or more combinations of D^* and T_i .

3. RESULTS OF FITTING FOR LARGE ASPECT ANGLES

In this section we consider some results of fitting EISCAT data with allowance for non-thermal effects; examples have been chosen to illustrate various features and problems of this kind of fit. In this paper we do not attempt to survey the occurrence of non-thermal plasma. However, it should be noted that we find significantly non-thermal plasma ($D^* > 0.5$) whenever the drift is large and that these effects are quite common in the auroral zone. We are currently preparing a series of publications on the results of our surveys of large data sets. However, in this paper, we have concentrated on a limited number of spectra to illustrate the principles involved. The data in this section were all obtained at large aspect angles. In Section 4 we will consider the problems associated with extending the analysis down to smaller aspect angles.

3.1. Results for 15 s integrated data

Spectra from the EISCAT U.K. Special Programme POLAR (VAN EYKEN *et al.*, 1984; WILLIS *et al.*, 1986) were fitted for the electron density, electron and ion temperatures and the non-Maxwellian distortion factor (N_e , T_e , T_i , D^*) assuming a 100% O^+ plasma. An example of an observed spectrum is shown in Fig. 5 together with the best Maxwellian and non-Maxwellian fits. The observed spectrum is from range gate 4 (centred on a range 750 km from Tromsø) and for the time period 06:35:45–06:36:00 UT on 27 October 1984. The observations are for a radar beam azimuth of 356° (cast of north) and an elevation of 21.5° , and at range gate 4 this line-of-sight subtends an angle of 72.0° with the geomagnetic field and is at an altitude of 311 km. At this time, the peak velocity of a sudden poleward flow burst was observed ($\sim 1.5 \text{ km s}^{-1}$). STBECK *et al.* (1989) have suggested that this was due to a big pulse in solar wind dynamic pressure observed by AMPTE-IRM shortly before it impinged upon the

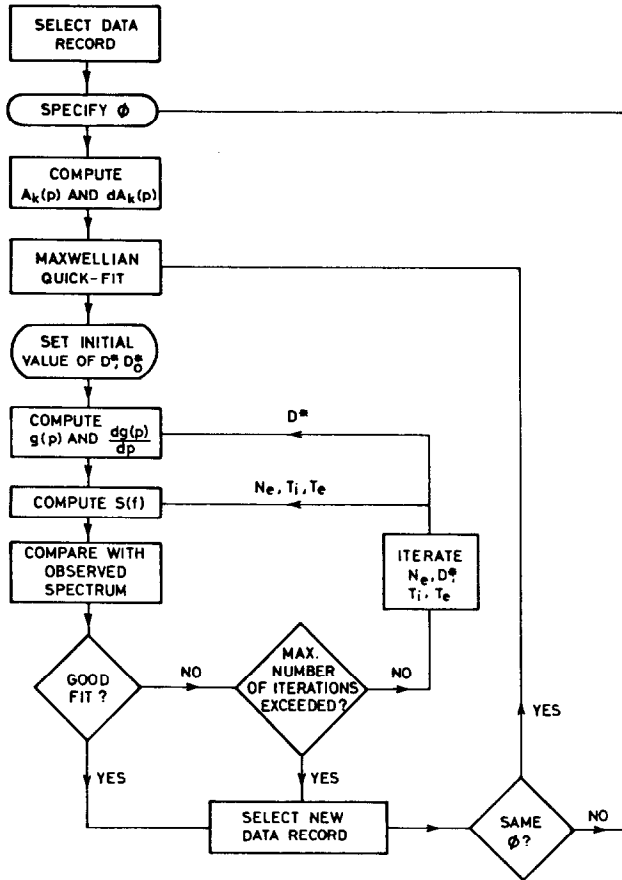


Fig. 4. Flowchart illustrating the non-Maxwellian data analysis procedure.

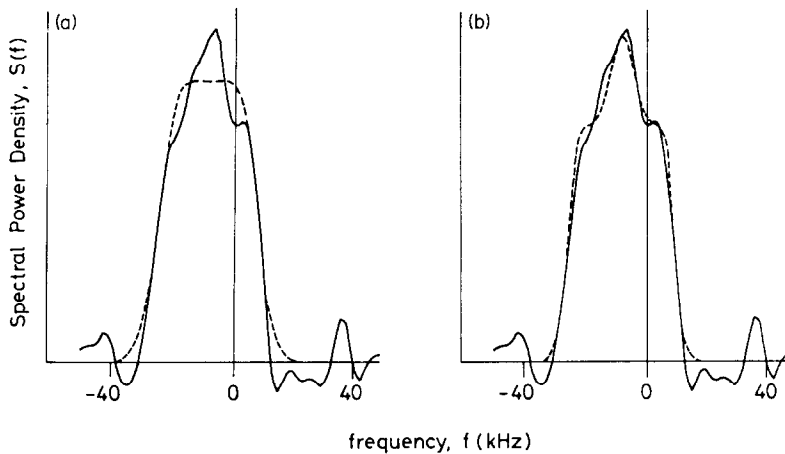


Fig. 5. A spectrum observed by the U.K. EISCAT Special Programme POLAR from range gate 4 and the time period 06:35:45–06:36:00 UT on 27 October 1984 (solid lines). For these data the line-of-sight subtends an angle of 72.0° with the geomagnetic field. The best Maxwellian and non-Maxwellian fits are shown by the dashed curves in parts (a) and (b), respectively.

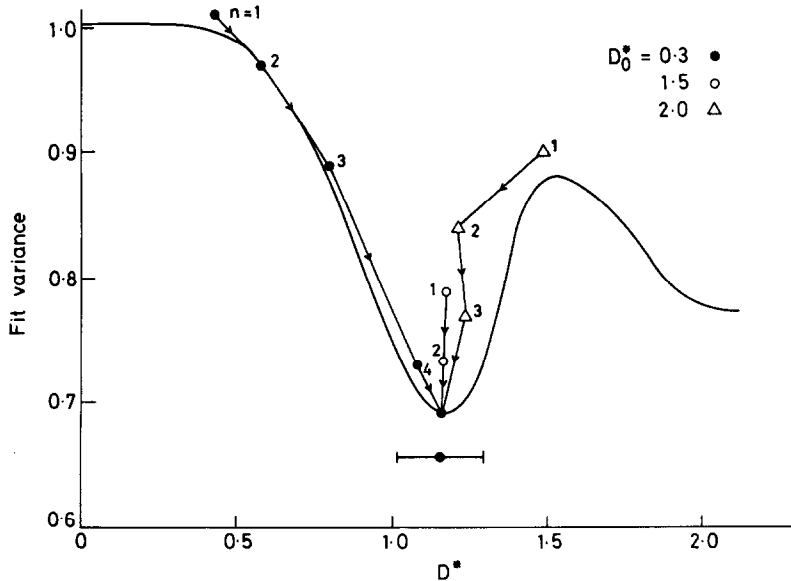


Fig. 6. Variance (arbitrary units) as a function of D^* for fits to the observed spectrum shown in Fig. 5. The curve shows the variation for three-parameter (N_e , T_e , T_i) fits (with fixed D^*) and the sequences of straight lines show three iteration paths for $D_0^* = 0.3$, 1.5 and 3.0 for 4-parameter (N_e , T_e , T_i , D^*) fits. The number of iterations to each point on a path is n . The error bar shows the computed error in D^* for converged four-parameter fits.

magnetopause, although TODD *et al.* (1986) have shown that this event is also consistent with the expected twin-vortex ionospheric signature of a flux transfer event at the dayside magnetopause. This spectrum is one of those used by LOCKWOOD *et al.* (1987) to show for the first time the effects of non-thermal ions on observed incoherent scatter spectra. The relation between the semi-empirical distortion parameter D^* and the ion drift Mach number D' for these data is discussed by LOCKWOOD *et al.* (1989a).

In order to quantify the improvement to the fit due to allowance for non-thermal effects, we have also carried out the three-parameter (N_e , T_e , T_i) fit using various (fixed) values of D^* . Figure 6 shows fit variance in arbitrary units (proportional to the sum of the squares of the fit residuals) as a function of the fixed value of D^* . The best fit corresponds to a clear minimum in fit variance, which is reduced to about 75% of its value at $D^* = 0$ (i.e. for a Maxwellian). Also shown in Fig. 6 are three iteration paths for three different values of D_0^* in the case of four-parameter (N_e , T_e , T_i , D^*) fits, the value of n beside each point giving the number of iterations to reach that point. In all three cases, the fits converge to the same point, the minimum of the three-parameter fit curve. Hence, the only effect of choosing an initial value for D^* , which is far from the correct value, is to increase slightly the number of iterations taken to reach a good fit and,

provided the maximum number of iterations allowed is not set to be too small, there is no need for some form of 'quick-fit' for D^* , as used for the other parameters. The curve in Fig. 6 does show that the fit variance begins to decrease again for very large D^* , as noted by MOORCROFT and SCHLEGEL (1988). However, no D_0^* value gave a four parameter fit corresponding to this region of parameter space, as illustrated by the example with $D_0^* = 2$ in Fig. 6. Results are not valid for $D^* > 3$, because approximations made in the SUVANTO (1988) algorithm begin to break down, and the only minimum found in the two-dimensional plane within the range $0 < D^* < 3$ is the one near $D^* = 1.25$.

3.2. Effects of post-integrating the data

The solid lines in parts (a) and (b) of Fig. 7 show the same observed spectrum with signatures typical of non-Maxwellian plasma. These data, which have been post-integrated over a period of 1 min (10:45:50–10:46:50 UT on 12 January 1988), are from the EISCAT experiment CP-4, which is identical to the POLAR experiment discussed in Section 3.1. except that data are recorded at intervals of 10 s rather than 15 s. The data are for the same scattering volume as discussed in the previous section, and hence the line-of-sight again makes an angle of 72.0° with the geomagnetic field. The spectrum presented in Fig. 7

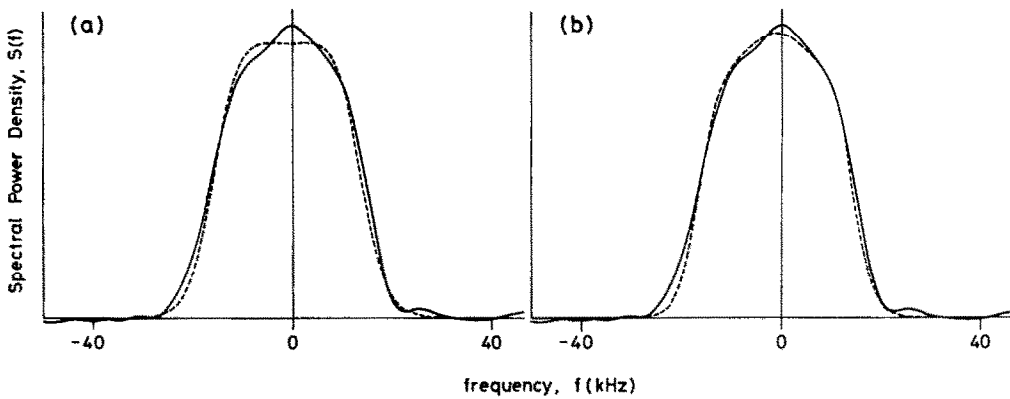


Fig. 7. Same as Fig. 5 for a spectrum observed by Common Programme CP-4 and post-integrated over a period of 1 min (10:45:50–10:46:50 UT on 12 January 1988).

was observed at the centre of a strong transient flow burst during which 55 kV of potential was applied across the EISCAT field of view (LOCKWOOD *et al.*, 1989b). These authors have provided very strong evidence that these flows are the result of a flux transfer event at the magnetopause.

The best Maxwellian and non-Maxwellian fits to the post-integrated data are also shown as dashed lines in parts (a) and (b), respectively. The fit appears to be much more satisfactory in (b). To quantify this visual impression, we have plotted the best-fit variance

for a three-parameter (N_e , T_e , T_i) fit as a function of the assumed value of D^* in Fig. 8. The variance has a clear minimum at $D^* = 0.89$, and the fit variance is reduced to about 30% of its value for $D^* = 0$. The percentage decrease in fit variance is much greater in this case than the previous one (Fig. 6), largely because the post-integration yields much lower random noise fluctuations (that is stochastic noise, as opposed to the background noise). Furthermore, the dependences of the plasma temperatures on D^* (Fig. 8) show clearly the fact that at $D^* = 0$ the ion tem-

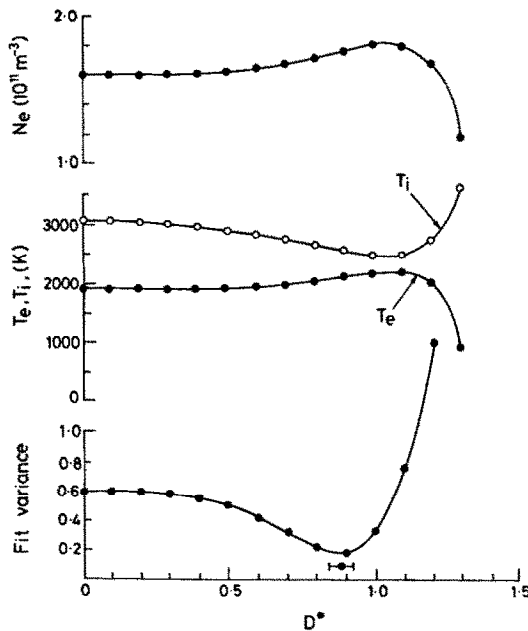


Fig. 8. Deduced electron density, plasma temperatures and the fit variance as a function of D^* for a three-parameter fit to the observed spectrum shown in Fig. 7.

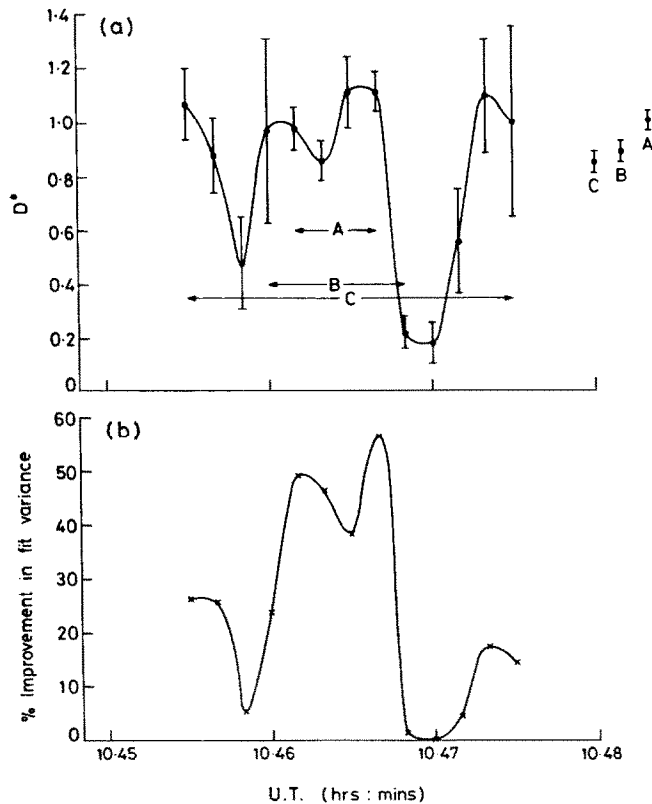


Fig. 9 (a) Values of D^* from fits to 10 s pre-integrated data for the antenna dwell period 10:45:25–10:47:35 on 12 January 1988. The D^* values corresponding to the periods (A), (B) and (C) are shown on the right. (N.B. the period (B) is that also studied in Figs. 7, 8 and 10). (b) The improvement (in %) in the variance for a four-parameter fit with allowance for non-Maxwellian effects over that for a Maxwellian, three-parameter fit.

perature is overestimated and the electron temperature underestimated for this large aspect angle, as discussed by RAMAN *et al.* (1981). Note that although the plasma is not highly non-Maxwellian, the electron temperature and density are underestimated by roughly 10% by assuming a Maxwellian, whereas the average ion temperature is overestimated by 20% in this example. Also shown in Fig. 6 and the bottom panel of Fig. 8 are the result of the four-parameter (N_e , T_e , T_i and D^*) fit, along with the error calculated by the fitting routine.

The post-integration can alter the deduced values of D^* because information about rapid variations in the plasma parameters is lost in the averaging process. This is illustrated in Fig. 9a, which shows D^* values of more than 1.0 deduced from fits to 10 s pre-integrated data for the antenna dwell period 10:45:25–10:47:35 UT. Two sudden and deep minima are apparent at 10:45:50 and 10:47:00 when the spectra return to double-peaked forms. To the right of the

figure are plotted the deduced D^* values corresponding to the post-integration periods (A), (B) and (C); here (B) is the period associated with Figs. 7 and 8. We presume that the minima in D^* reflect rapid reductions in the plasma drift velocity. It should be remembered, however, that the theoretical ion velocity distribution function employed in the fitting procedure was originally derived assuming a steady state (see ST.-MAURICE and SCHUNK, 1979). This approach can be justified if the typical time scale associated with temporal variations is much larger than the relaxation time associated with ion-neutral collisions, which drive the non-thermal velocity distribution. Assuming that the collision frequency is of the order of 1 s^{-1} , we conclude that the present fitting procedure may yield inaccurate results if significant temporal variations occur in time scales of the order of 1 s or less. It is interesting to note that the D^* values for fitting post-integrated data are very close to the averages of the results of fits to 10 s data, but the error bars are very

much smaller in the former case as the effects of stochastic noise are reduced. However, we note that, although not true of this case, we frequently find examples where post-integrating the data over periods of several minutes causes the fit to fail, whereas fits to shorter periods (<1 min) do not fail despite their higher random noise levels. From tristatic EISCAT observations, we find that this is caused by large variability in the drift giving fluctuations in D^* which are considerably greater than those in Fig. 9. Post-integrating over such D^* fluctuations causes distorted spectra and the fit fails to converge.

Part (b) of Fig. 9 shows the percentage improvement in fit variance achieved by non-Maxwellian (four-parameter) fits to the 10 s data compared with that for a Maxwellian (three-parameter) fit. The significance of the decrease must be assessed for each fit separately, but in every case the fit is improved by the non-Maxwellian analysis, as expected because of the addition of a degree of freedom. Note that the relative improvement is small for $D^* < 0.5$, hence in this range only low-noise spectra can be distinguished from the shape for a Maxwellian distribution. The smallest D^* which can be resolved as significantly different from a Maxwellian is therefore decreased by post-integration.

3.3. Fits allowing for mixed ion composition

In the case of two ion species, we have as many as seven free parameters for which we would ideally fit: ion composition, $N(\text{O}^+)/N_e$; electron density, N_e ; electron temperature, T_e ; two ion temperatures, T_{i1} and T_{i2} ; and two non-Maxwellian distortion factors, D_1^* and D_2^* . As a result, obtaining a unique fit is very much more difficult than in the single species case. We employ one or both of two approaches to this problem. First, theory can be evoked to obtain some relation between certain parameters and hence reduce their number. Second, one can fit for a fixed value of one of the parameters, ion composition, say, then fit again for a different composition and search for a minimum in variance.

Figure 10 illustrates an attempt to determine ion composition for the spectrum shown in Fig. 7, with the assumption that the three-dimensional ion temperatures are equal for the two species ($T_{i1} = T_{i2}$). This assumption is valid when the ion-neutral frictional heating term in the ion energy balance equation is dominant. This is because this term is proportional to the neutral mass but largely independent of the ion species (ST.-MAURICE and SCHUNK, 1979). However, the molecular ions will usually have a lower D^* , even if they are of the same temperature, as observed by

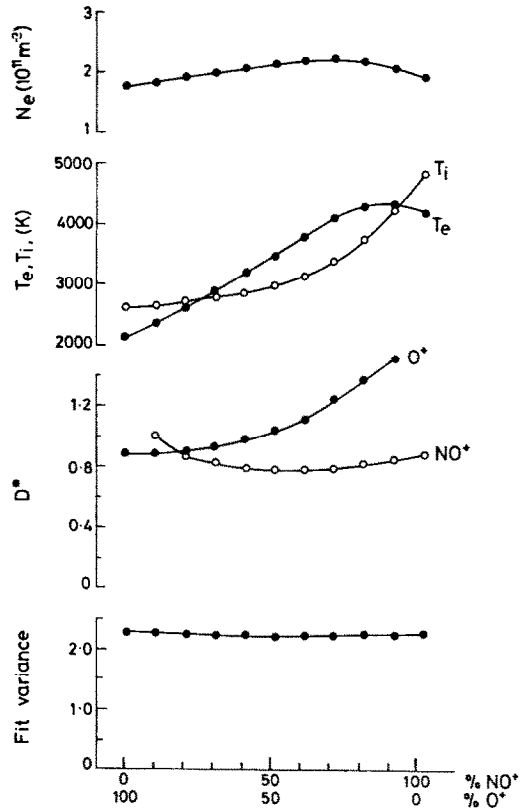


Fig. 10. Deduced electron density, plasma temperatures, values of D^* and fit variance for five-parameter (N_e , T_e , T_i , D_1^* , D_2^*) fits to the observed spectrum shown in Fig. 7 and plotted as a function of the assumed ion composition.

ST.-MAURICE *et al.* (1976), because NO^+ ions, in particular, undergo mainly elastic polarization scatter interactions rather than the resonant charge exchange interactions O^+ can have with O, the latter being much more efficient at producing a non-thermal ion distribution. An interesting exception to this has recently been pointed out by WINSER *et al.* (1989), in that any N_2^+ ions will tend to have a higher D^* . In general, therefore, D_1^* and D_2^* must be kept as separate variables.

Figure 10 shows the results of five-parameter fits (N_e , T_e , T_i , $D^*(\text{O}^+)$ and $D^*(\text{NO}^+)$ for various (fixed) ion compositions. We assume the molecular ions are NO^+ , as that is the most likely species, and the spectrum will be virtually identical to that for O_2^+ or N_2^+ , or a mixture of the three, for the same distortion of the distribution function, D^* . Although the fit variance is practically constant and the composition thus remains unknown, we are left with an important conclusion: performing the spectral analysis under the assumption

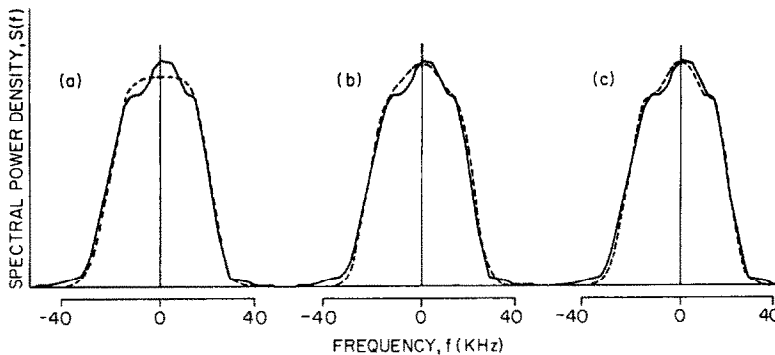


Fig. 11. An example of a spectrum observed by the EISCAT CP-3-E experiment (solid line in each part of the figure) compared with the best (a) Maxwellian, (b) non-Maxwellian pure O^+ fit and (c) non-Maxwellian, mixed composition fit. These data were recorded in scan position 5 of the scan between 1300 and 1330 UT on 27 August 1986, and were integrated over the 100 s dwell period of the radar in this position.

of a 100% O^+ ion gas yields a lower limit for the value of $D^*(O^+)$ in this case. In other words, allowing for a molecular ion component acts to increase the D^* estimate for O^+ . In our example $D^*(O^+) > 0.89$, and the non-thermal nature of the plasma is thus confirmed although the ion composition remains ambiguous. It should be remembered that the analysis was carried out assuming that the ion temperatures for both species were equal. However, we expect the above conclusion to be more general. For instance, suppose that a spectrum has been fitted with 100% O^+ , and we wish to repeat the procedure allowing for a minor molecular component NO^+ . Now, $D^*(NO^+)$ is likely to be less than $D^*(O^+)$ as found by ST.-MAURICE *et al.* (1976) from AE-C RPA data. As a result, it seems natural to assume that the presence of a molecular ion component (which is less non-thermal than O^+) in our analysis must be effectively cancelled by a rise in $D^*(O^+)$ to obtain the same degree of distortion in the spectrum as in the case of pure O^+ . This idea is supported by the results of similar analysis for other, fixed values of the ratio of the ion temperatures for the two species. Note that other theoretical approaches could be adopted. For example, if it is assumed that the dominant molecular species is NO^+ and that it suffers predominantly polarization interactions and no resonant charge exchange, the results of BARAKAT *et al.* (1983) could possibly be used to fix the ratio $D^*(O^+)/D^*(NO^+)$.

Figure 11 shows a spectrum observed by the EISCAT CP-3-E experiment (see the following section) which does give a pronounced minimum in the fit variance-ion composition curve for a five-parameter fit, equivalent to that shown in Fig. 10. Also shown are the results for (a) a Maxwellian (three-parameter) fit, (b) a non-Maxwellian, single species

(O^+) fit and (c) a non-Maxwellian fit with the molecular composition of 25% ($N(O^+)/N_e = 0.75$) and with equal ion temperatures. The solid line corresponds to the observed spectrum and the dashed line denotes the theoretical ones in each part of the figure. The fit variances for these three fits are 2.0, 0.9 and 0.6 (arbitrary units), respectively. Hence the fit variances support quantitatively the visual improvement to the fit obtained by introducing non-thermal, mixed species plasma in this case. The implications of these data have been discussed in more detail by WINSER *et al.* (1989). Supporting evidence for the validity of this mixed species fit comes from the fact that it is the only one to give a realistic electron temperature profile. However, we note that this case is very unusual in that the D^* value derived for the molecular species is higher than that for the O^+ ions, and theoretically this is not expected, at least not for NO^+ ions. As a result, WINSER *et al.* (1988) have suggested that the molecular ions in this case were N_2^+ . In the majority of cases we have studied, the ion composition cannot be determined, and LOCKWOOD *et al.* (1989a) and WINSER *et al.* (1989) have pointed out that this is almost certainly because the spectra are usually ambiguous when D^* is lower for the molecular species than for O^+ , as is expected for NO^+ molecular ions.

4. APPLICATION TO OBSERVATIONS OVER A RANGE OF ASPECT ANGLES

One shortcoming of the ion velocity distribution function employed by RAMAN (1980) and SUVANTO (1988) is the fact that no distortions from a Maxwellian shape are allowed for in the field-parallel direction. The use of this model also sets limitations to the data analysis procedure: technically speaking, if we let the

aspect angle tend to zero, the functional dependence of the line-of-sight ion velocity distribution on O^+ disappears (see RAMAN *et al.*, 1981) so that no information of non-thermal effects can be obtained by studying the plasma in the field-parallel direction only. In practice, the problem is present for small enough aspect angles. We stress that this is a feature of the model used rather than a reflection of real plasma behaviour, although spectral noise may result in this being the case for more general forms of the distribution function if non-Maxwellian spectral signatures are small for the field-parallel direction.

To illustrate this point, data for each of the aspect angles studied by the EISCAT CP-3-E experiment (the latitude scanning program discussed, e.g. by WINNER *et al.*, 1987, 1989) were fitted for the parameters N_e , D^* , T_e and T_i assuming an ion gas consisting of 100% O^+ ions. Figure 12 shows the results of 21 fits (corresponding to 21 different values of D_0^* between 0.0 and 2.0) for each scan position. For the aspect angle of 2.5° the deduced values of D^* are scattered between 0 and a highly unrealistic value of about 4, so that no conclusions regarding the correct value can be drawn within the set maximum number of iterations (20). Around 20° , the determination of D^* becomes possible. However, the choice of D_0^* still plays a minor role for aspect angles up to about 50° : if D_0^* is too small the analysis programme will still not have reached the correct answer for both T_i and D^* , within the set number of maximum iterations. Finally, for aspect angles larger than about 50° , the correct value of D^* is always obtained, regardless of D_0^* ,

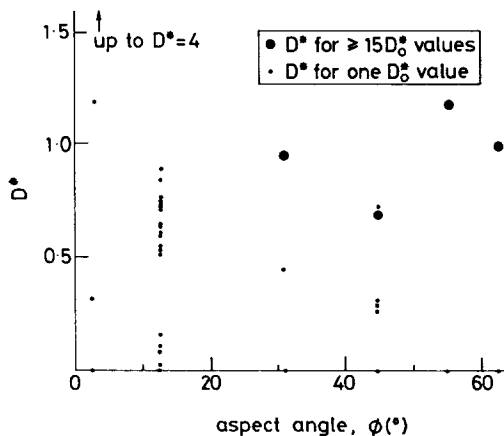


Fig. 12. Values of D^* from 21, four-parameter fits corresponding to 21 different values of D_0^* between 0.0 and 2.0 for various aspect angles. The data are from the EISCAT Common Programme CP-3-E and were recorded in the latitude scan between 1300 and 1330 UT on 27 August 1986.

provided that the analysis is not commenced with $D_0^* = 0$. The range of aspect angles over which fits can be obtained can be increased by increasing the maximum allowed number of iterations. However, fits for zero aspect angle will never be possible as there is no information on D^* in the theoretical spectrum used here. At aspect angles close to zero, the effect of D^* on the spectrum will be very small and could easily be masked by spectral noise. Hence, the minimum aspect angle is a function of the stochastic noise in the spectrum and the maximum number of iterations: the value we have quoted is probably quite low as these are unusually 'clean' spectra. This problem is expected to still apply to any more general ion velocity distribution functions which may be devised in the future, as it is highly unlikely that there will be sufficient information to allow field-parallel observations to be extrapolated to give information on the velocity distribution at large aspect angles.

A small value of the aspect angle does not prevent the determination of the line-of-sight ion temperature. Generally speaking, in order to deduce the average ion temperature, a measure of the random kinetic energy of the ions, it is necessary to extrapolate to directions away from the line-of-sight using an assumed form of the velocity distribution function.

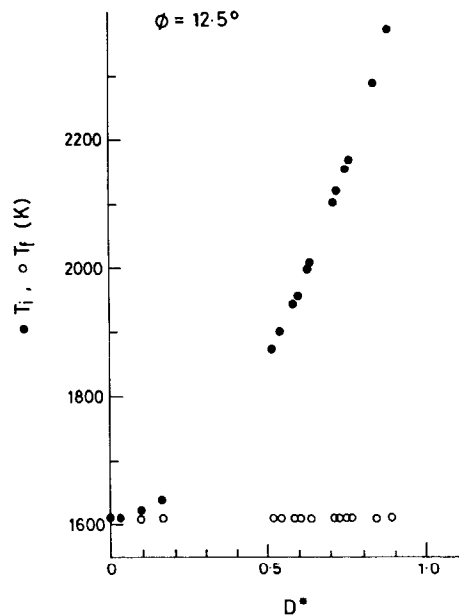


Fig. 13. Values of the three-dimensional ion temperature (T_i) and one-dimensional line-of-sight ion temperature (T_l) as a function of fitted D^* value, each point corresponding to different values of D_0^* , for the spectrum observed at an aspect angle of 12.5° in the data shown in Fig. 12.

For the RAMAN (1980) distribution function used here, D^* cannot be determined and hence this extrapolation cannot be made if the aspect angle is small. This effect can be seen from Fig. 13: the analysis always yields correct values for the line-of-sight temperature but using a variety of combinations for D^* and T_i values to obtain exactly the same quality fit in each case. This is a matter of importance since it is the average (or three-dimensional) temperature which characterises the ions whenever energy arguments (for example in the frictional heating equation) are used. It is stressed that even if the spectrum is the familiar double humped one, typical of thermal plasma for small aspect angles, the ion temperature deduced by the isotropic Maxwellian interpretation should not be used (e.g. when using the ion energy balance equation to study frictional heating) if limits to the effects of non-thermal plasma cannot be defined by other means. Also, any results of non-Maxwellian analysis at low aspect angles must be assessed very critically because the shape of the theoretical spectrum is insensitive to variations in D^* , as discussed above.

5. CONCLUSIONS

We have discussed a procedure for analysing incoherent scatter spectra from non-thermal F -region plasma. The method has been applied to data from the EISCAT Special Programme POLAR and Common Programmes CP-4 and CP-3-E, and it has been found that in cases where non-Maxwellian effects are expected, the fit variance is generally much lower than for the standard analysis. The iterative method of

fitting was repeated varying the initial value of the shape distortion parameter D^* , and the result is independent of this initial value in all cases where the aspect angle exceeds about 50° . However, the fact that the theoretical spectrum is insensitive to non-Maxwellian distortions when the aspect angle is small makes the determination of D^* and the average ion temperature increasingly more difficult when the plasma is viewed at a small angle ($<10\text{--}15^\circ$) with respect to the magnetic field. Regarding the ion gas as thermal (because of the double-humped shape of the spectrum) and the deduced line-of-sight temperature as the average temperature may lead to serious errors if, for example, this value of the temperature is used in association with energy arguments, such as in the frictional heating equation.

Spectra were also fitted allowing for different ion compositions with the assumption that the average ion temperatures were equal. Although in the vast majority of attempted cases we were unable to determine the ion composition, it was found that the D^* values for O^+ were increased by assuming that molecular ions were present. In particular, all the large D^* values deduced assuming a single ion species can be considered as lower limits, confirming that the plasma was indeed non-thermal.

Acknowledgements—We thank the director and staff of EISCAT for their help. EISCAT is supported by the French CNRS, West German MPG, Swedish NFR, Norwegian NAVF, Finnish SA and British SERC. K. S. is supported by the Oskari Huttenen Foundation of Finland, with assistance from an ORS scholarship and the Academy of Finland. We also thank S. W. H. COWLEY, J.-P. ST.-MAURICE and D. M. WILLIS for their comments and advice and S. R. CROTHERS and V. N. DAVDA for assistance with software and graphics.

REFERENCES

- | | | |
|---|-------|---|
| BARAKAT A. R., SCHUNK R. W.
and ST.-MAURICE J.-P. | 1983 | <i>J. geophys. Res.</i> 88 , 3237. |
| BUCHERT S. and LA HOZ C. | 1988 | <i>Nature</i> 333 , 438. |
| EVANS J. V. | 1969 | <i>Proc. IEEE</i> 57 , 496. |
| KIKUCHI K., ST.-MAURICE J.-P. and BARAKAT A. R. | 1988 | <i>Annales. Geophys.</i> 7 , 183. |
| LOCKWOOD M. and WINSER K. J. | 1988 | <i>Planet. Space Sci.</i> 36 , 1295. |
| LOCKWOOD M., BROMAGE, B. J. I., HORNE R. B.,
ST.-MAURICE J.-P., WILLIS D. M. and
COWLEY S. W. H. | 1987 | <i>Geophys. Res. Lett.</i> 14 , 111. |
| LOCKWOOD M., SUVANTO K., ST.-MAURICE J.-P.,
KIKUCHI K., BROMAGE B. J. I., WILLIS D. M.,
CROTHERS S. R., TODD H. and COWLEY S. W. H. | 1988 | <i>J. atmos. terr. Phys.</i> 50 , 467. |
| LOCKWOOD M., SUVANTO K., WINSER K. J.,
COWLEY S. W. H. and WILLIS D. M. | 1989a | <i>Adv. in Space Res.</i> 9 (5), 113. |
| LOCKWOOD M., SANDHOLT P. E. and COWLEY S. W. H. | 1989b | <i>Geophys. Res. Lett.</i> 16 , 33. |
| MOORCROFT D. | 1964 | <i>J. geophys. Res.</i> 69 , 955. |
| MOORCROFT D. and SCHLEGEL K. | 1988 | <i>J. atmos. terr. Phys.</i> 50 , 455. |
| RAMAN R. S. V., ST.-MAURICE J.-P. and ONG R. S. B. | 1981 | <i>J. geophys. Res.</i> 86 , 4751. |
| SIBECK D. G., BAUMJOHANN W. and LOPEZ R. E. | 1989 | <i>Geophys. Res. Lett.</i> 16 , 13. |

- ST.-MAURICE J.-P., HANSON W. B. and WALKER J. C. G. 1976 *J. geophys. Res.* **81**, 5438.
 ST.-MAURICE J.-P. and SCHUNK R. W. 1979 *Rev. Geophys. Space Phys.* **17**, 99.
 SUVANTO K. 1988 *Radio Sci.* **23**, 989.
 TODD H., BROMAGE B. J. I., COWLEY S. W. H.,
 LOCKWOOD M., VAN EYKEN A. P. and
 WILLIS D. M. 1986 *Geophys. Res. Lett.* **13**, 909.
 VAN EYKEN A. P., RISHBETH H., WILLIS D. M.
 and COWLEY S. W. H. 1984 *J. atmos. terr. Phys.* **46**, 635.
 WILLIS D. M., LOCKWOOD M., COWLEY S. W. H.,
 VAN EYKEN A. P., BROMAGE B. J. I., RISHBETH H.,
 SMITH P. R. and CROTHERS S. R. 1986 *J. atmos. terr. Phys.* **48**, 987.
 WINSER K. J., LOCKWOOD M. and JONES G. O. L. 1987 *Geophys. Res. Lett.* **14**, 957.
 WINSER K. J., LOCKWOOD M., JONES G. O. L.
 and SUVANTO K. 1989 *J. geophys. Res.* **94**, 1439.
- Reference is also made to the following unpublished material:*
- LEJEUNE G. 1979 EISCAT technical note 79/18.
 RAMAN R. S. V. 1980 Thesis, University of Michigan, U.S.A.